Expanded View Figures

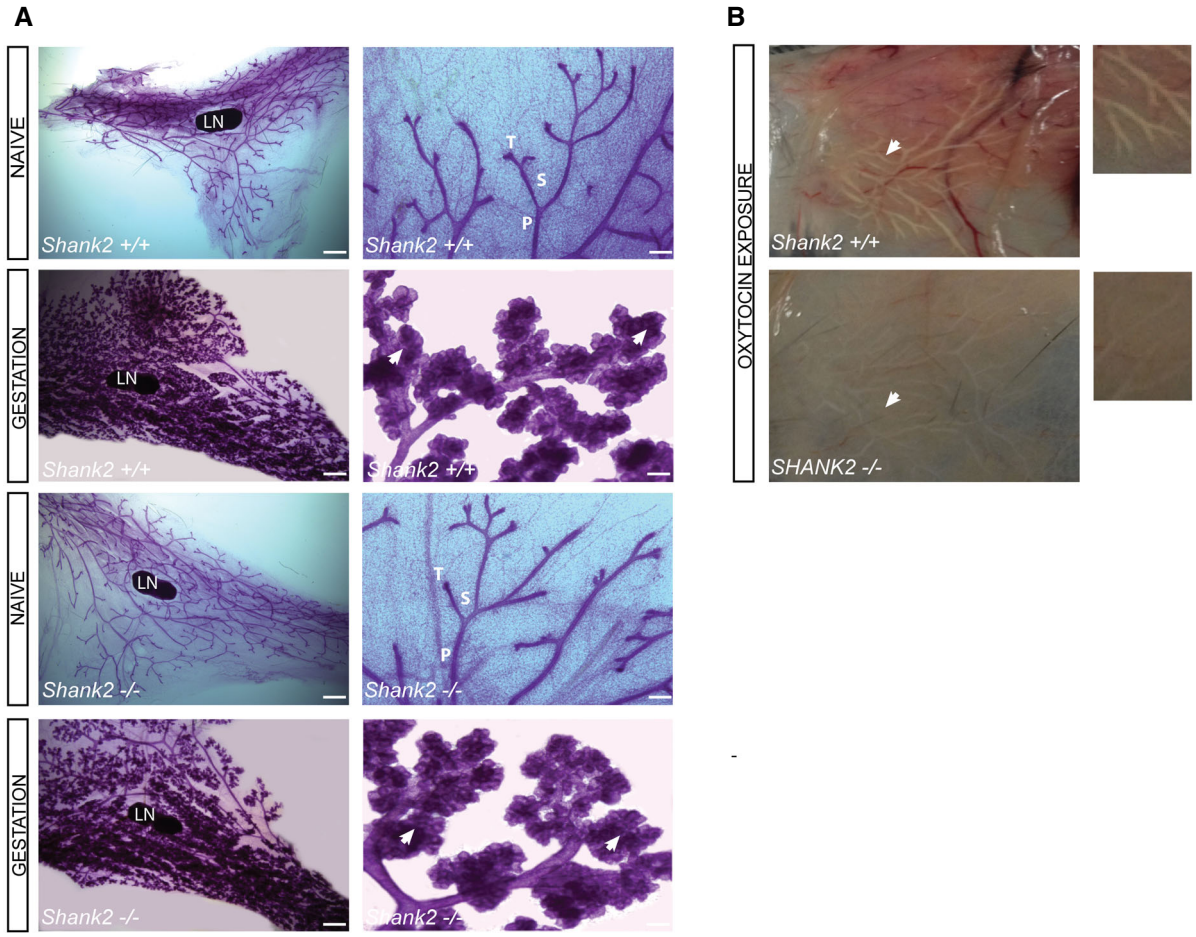

Figure EV1. *Shank2*$^{-/-}$ mice develop functionally and morphologically normal mammary glands.

A Carmine-stained whole-mount preparations of mammary glands of the fourth inguinal gland isolated from naive and pregnant (1 day before delivery) *Shank2*$^{+/+}$ and *Shank2*$^{-/-}$ mice. Images shown are representatives of three mice per genotype at the age of 8 weeks. Scale bars: 2 mm whole mount (left panel); 200 μm in higher magnifications (right panel). Mammary glands of naive *Shank2*$^{-/-}$ mice (upper panel) showed no gross abnormalities in ductal morphogenesis in comparison with *Shank2*$^{+/+}$ mice. Additionally, during gestation (lower panel), *Shank2*$^{-/-}$ mice developed normal lobuloalveolar structures (arrowheads) intended for milk production. LN, lymph node; P, primary duct; S, secondary branch; T, side branch.

B Functional assessment of the mammary glands in *Shank2*$^{+/+}$ and *Shank2*$^{-/-}$ dams. Milk transport and milk secretion from the alveoli into the mammary gland ducts were induced by myoepithelial contraction trigged through treatment with oxytocin. Representative images of thoracic gland #2–3, isolated from *Shank2*$^{+/+}$ (upper panel) and *Shank2*$^{-/-}$ mice (lower panel) 1 day before delivery. Mammary glands were incubated for 1 min with (1 mg/ml) oxytocin. After 1 min, images were taken for the visualization of milk ejection in the mammary gland ducts. Both genotypes displayed milk ejection after oxytocin exposure.

Figure EV2. *Shank2*$^{-/-}$ mice display no anxiety-related behavior or social avoidance during pup presentation.

A Representative illustration of the pup interaction zones and corner zones. Time spent in pup interaction zone and corner zone was measured during the first 2 min of social investigation in the pup retrieval test (trial 1) in *Shank2*$^{+/+}$ and *Shank2*$^{-/-}$ mice.

B Left diagram: No significant difference was detected comparing time spent in pup interaction zones (unpaired two-tailed Student's *t*-test, $P = 0.7090$), and corner zones (unpaired, two-tailed Student's *t*-test, $P = 0.4597$). Right diagram: Representative heat map tracings of *Shank2*$^{+/+}$ and *Shank2*$^{-/-}$ mice. Hot colors indicate more time spent in a specific area, while cool colors represent less amount of time.

C Left diagram: Sample behavior raster blot showing average duration *Shank2*$^{+/+}$ and *Shank2*$^{-/-}$ spent in pup interaction zones. Right diagram: No significant difference was detected comparing the average duration *Shank2*$^{+/+}$ and *Shank2*$^{-/-}$ mice spent in the pup interaction zones (Mann–Whitney test, $P = 0.3865$).

D No significant difference was detected comparing the time spent freezing between *Shank2*$^{+/+}$ and *Shank2*$^{-/-}$ mice (two-tailed Student's *t*-test, $P = 0.8329$).

E Tracking paths of *Shank2*$^{+/+}$ and *Shank2*$^{-/-}$ mice during the first 2 min of social exposure toward the pups.

F No significant difference was detected comparing the average movement velocity when *Shank2*$^{+/+}$ and *Shank2*$^{-/-}$ mice did not engage in maternal behavior (trial 5, test day) (Mann–Whitney test, $P = 0.8633$). All graphs are presented as mean ± SEM, $^{*}P < 0.05$, $^{**}P < 0.01$, $^{***}P < 0.001$. *Shank2*$^{+/+}$ $n = 9$, *Shank2*$^{-/-}$ $n = 9$.

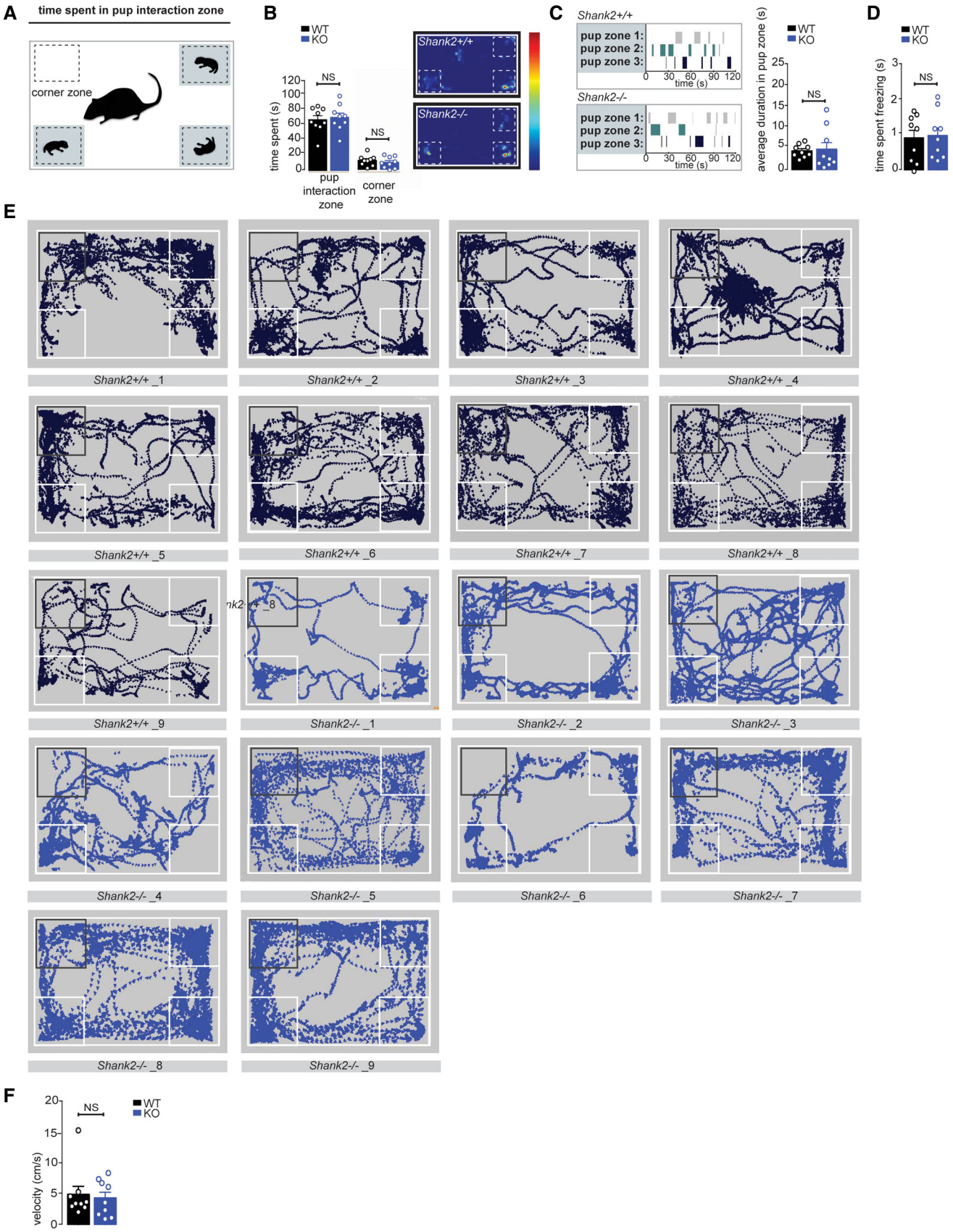

Figure EV2.

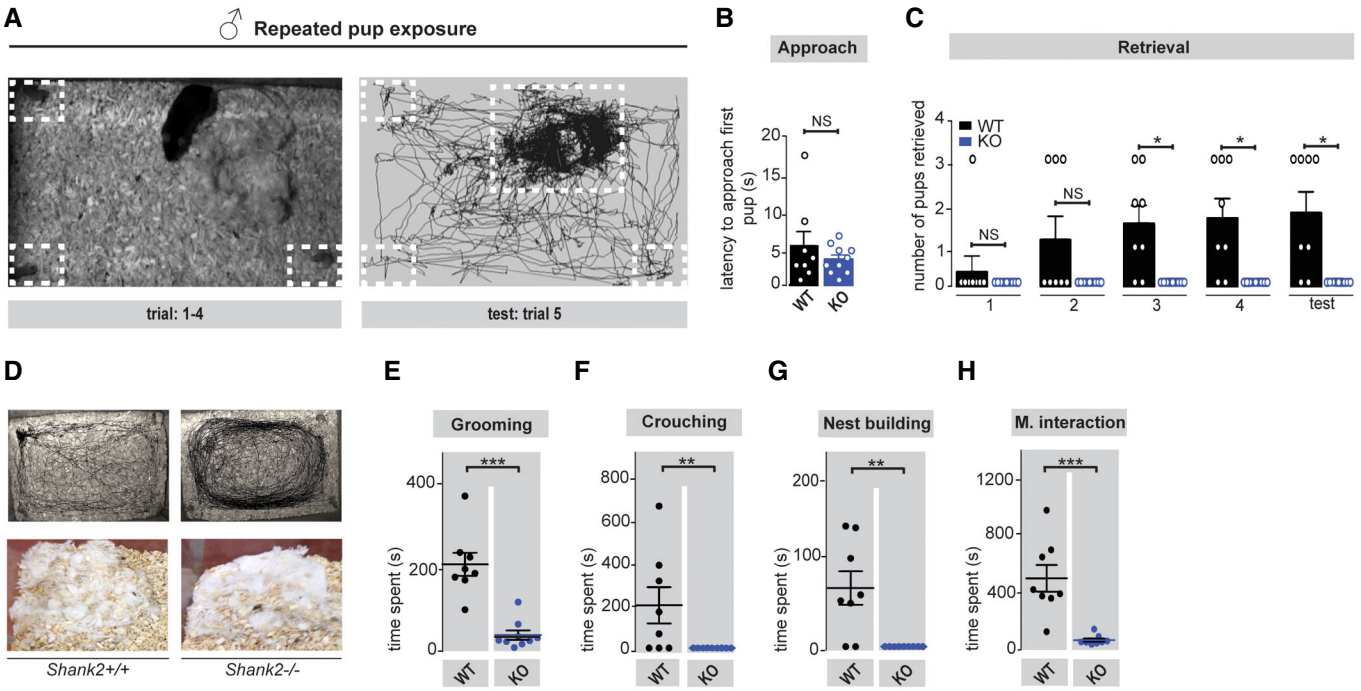

Figure EV3. Social bonding behavior of male *Shank2*$^{-/-}$ mice cannot be induced by social pup exposure.

A Left panel: Maternal behavior can be induced in male mice through repeated social exposure to pups (trial 1–5). After repeated pup exposure (right panel), male mice started to retrieve pups and displayed maternal behavior by crouching over the pups, thereby becoming more attached to the nest location as displayed in the tracking path (right panel).

B No significant difference was detected in the latency to approach the provided pups between *Shank2*$^{+/+}$ and *Shank2*$^{-/-}$ male mice, Mann–Whitney test, $P = 0.662$.

C Pup-exposed male *Shank2*$^{-/-}$mice failed to become attached toward the pups after repeated exposure, as demonstrated by the failure to retrieve pups during trial 1–5 compared to *Shank2*$^{+/+}$ males, two-way mixed ANOVA, effect of genotype: $^{**}P < 0.003$, effect of trial: $^{*}P = 0.032$, trial × genotype interaction: $^{*}P = 0.032$.

D–H Upper panel: Representative tracking path of *Shank2*$^{+/+}$ and *Shank2*$^{-/-}$ male mice during exposure to pups in the 20 min test session (trial: 5). *Shank2*$^{+/+}$ males spent the majority of their time on the nest location crouching over the pups; *Shank2*$^{-/-}$ males displayed no preference for the nest location, or participate in nest building activity (lower panel). Additionally, all major components of maternal care responses (E) pup grooming, Mann–Whitney test, $^{***}P < 0.001$, (F) crouching, Mann–Whitney test, $^{**}P = 0.007$, (G) nest building, Mann–Whitney test, $^{**}P = 0.002$, (H) paternal interaction, Mann–Whitney test, $^{***}P < 0.001$, were significantly reduced in *Shank2*$^{-/-}$ male mice. All graphs are presented as mean ± SEM, $^{*}P < 0.05$, $^{**}P < 0.01$, $^{***}P < 0.001$. *Shank2*$^{+/+}$ $n = 8$, *Shank2*$^{-/-}$ $n = 9$.

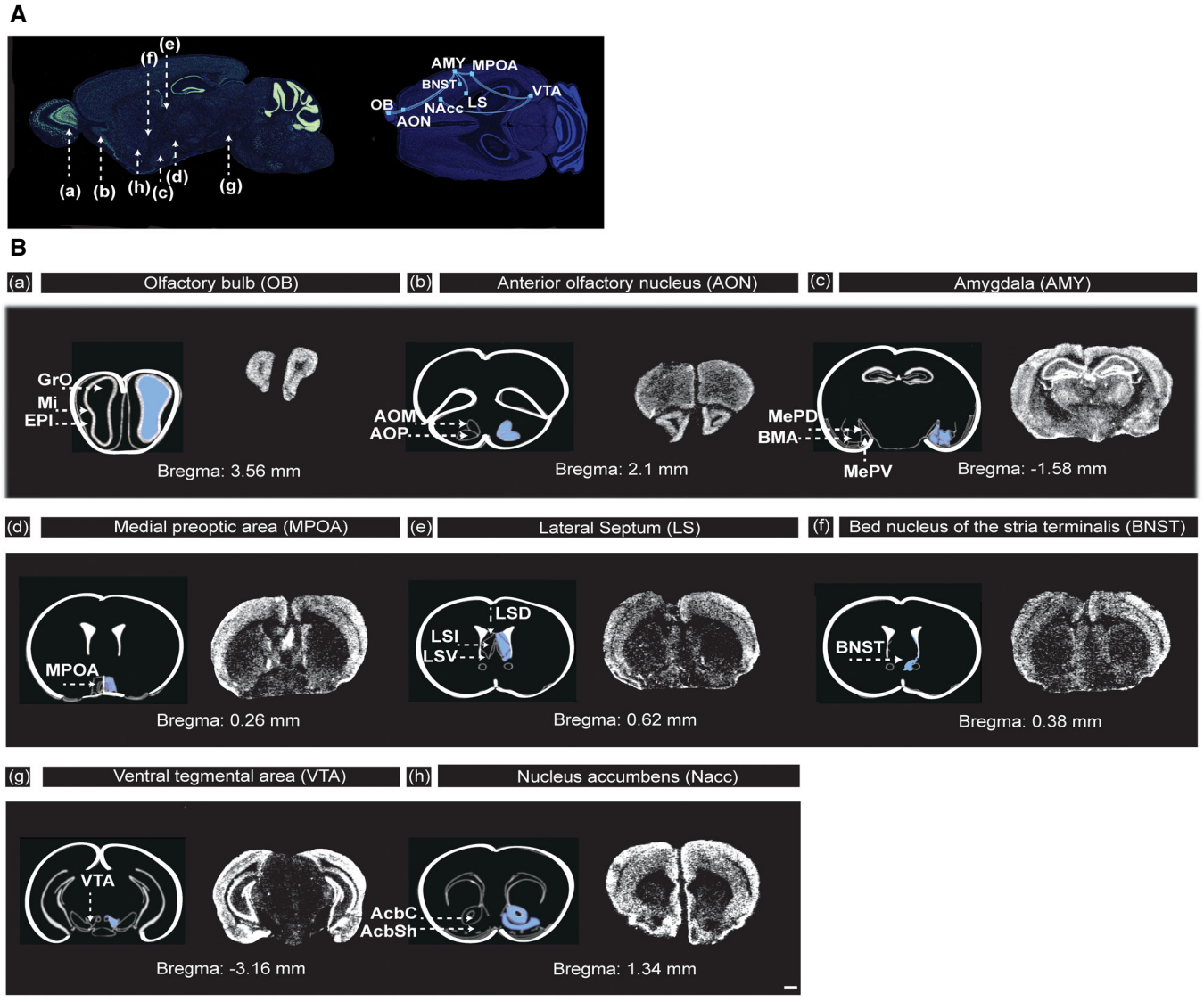

Figure EV4. *Shank2* mRNA is moderately expressed in the circuit areas regulating social attachment behavior.

A Representative illustration of the neuronal pathway (a–g) involved in the regulation of social attachment behavior. (a) OB, olfactory bulb; (b) AON, anterior olfactory nucleus; (c) AMY, amygdala; (d) MPOA, medial preoptic area; (e) LS, lateral septum, (f) BNST, bed nucleus of the stria terminalis, (g) VTA, ventral tegmental area; (h) NAcc, nucleus accumbens.

B (a–h) Distribution of *Shank2* mRNAs in major core regions of the neuronal circuit responsible for the regulation of social attachment behavior. Images shown are coronal brain sections (16 μm) of 8-week-old *Shank2*$^{+/+}$ mice, scale bar: 1 mm. *In situ* hybridization results indicated the expression levels of *Shank2* in the (a) olfactory bulb (c) amygdala and (h) nucleus accumbens. GrO, granular cell layer of the olfactory bulb; Mi, mitral cell layer of the olfactory bulb; EPI, external plexiform layer of the olfactory bulb; AOM, anterior olfactory nucleus medial part; AOP, anterior olfactory nucleus posterior part; MePD, medial amygdaloid nucleus; BMA, basomedial amygdaloid nucleus, anterior part; MPOA, medial preoptic area; LSD, lateral septal nucleus, dorsal part; LSI, lateral septal nucleus, intermediate part; LSV, lateral septal nucleus, ventral part; BNST, bed nucleus of the stria terminalis; VTA, ventral tegmental area; AcbC, accumbens nucleus, core; AcbSh, accumbens nucleus, shell.

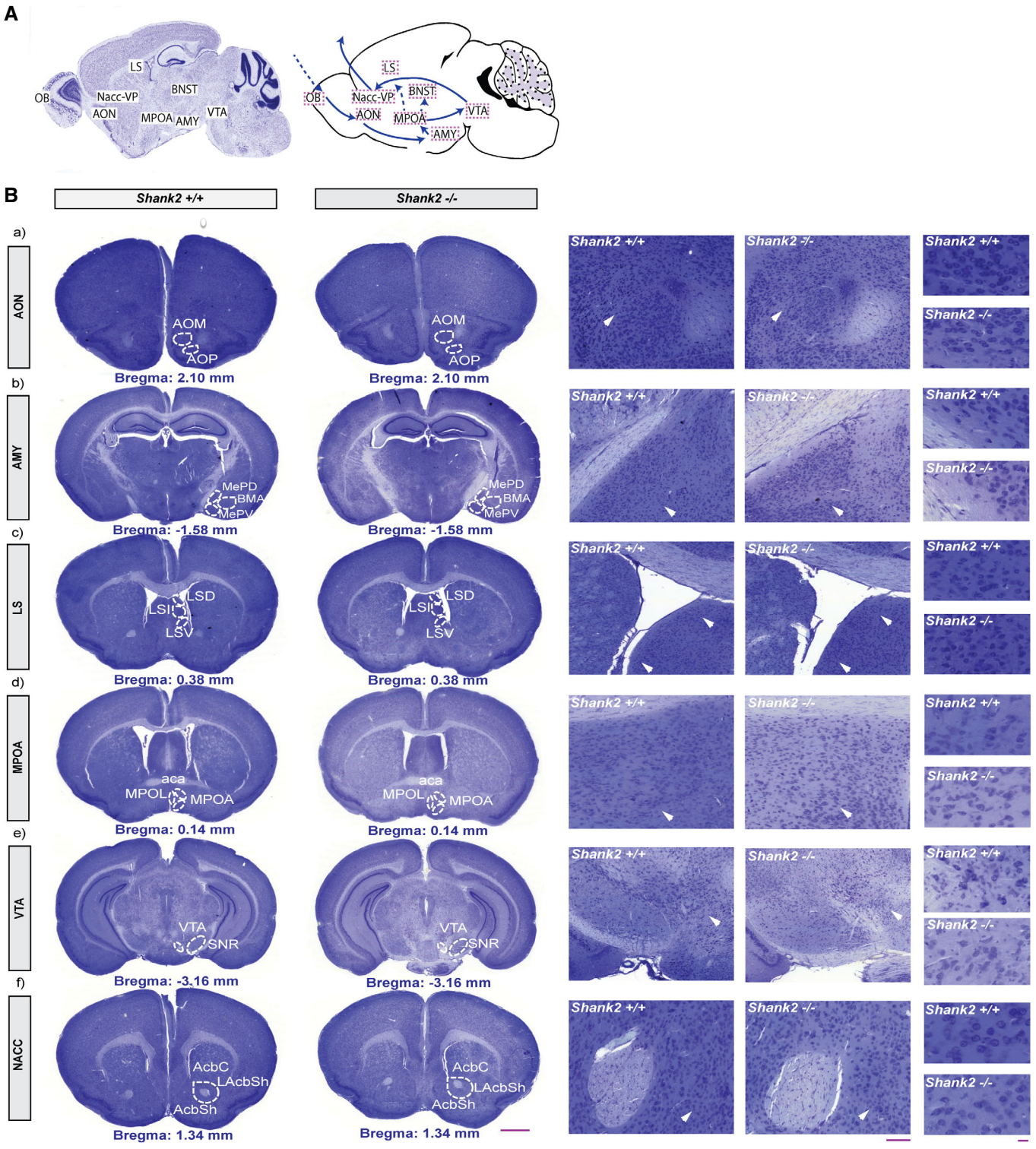
A
LS
BNST
OB
Nacc-VP
AON
MPOA
AMY
VTA
B
Shank2 +/+
Shank2 -/-
a)
AON
AOM
AOP
Bregma: 2.10 mm
b)
AMY
MePD
BMA
MePV
Bregma: -1.58 mm
c)
LS
LSD
LSI
LSV
Bregma: 0.38 mm
d)
MPOA
aca
MPOL
MPOA
Bregma: 0.14 mm
e)
VTA
VTA
SNR
Bregma: -3.16 mm
f)
NACC
AcbC
LAcbSh
AcbSh
Bregma: 1.34 mm

Figure EV5.

Figure EV5. *Shank2*$^{-/-}$ mice display no gross abnormalities in the cytoarchitectonic organization of the circuit areas regulating social attachment behavior.

A Representative illustration of the neuronal pathway regulating social attachment behavior in mice. (a) OB, olfactory bulb; (b) AON, anterior olfactory nucleus; (c) AMY, amygdala; (d) MPOA, medial preoptic area; (e) LS, lateral septum, (f) BNST, bed nucleus of the stria terminalis, (g) VTA, ventral tegmental area; (h) NAcc, nucleus accumbens.

B Circuit-specific comparison of the brain morphology between *Shank2*$^{+/+}$ and *Shank2*$^{-/-}$ mice in low (left panel) and high (right panel) magnification view (a–f). Scale bars: 1 mm coronal section, 100 μm left magnification, 20 μm right magnification. Nissl-stained coronal brain sections (16 μm) show similar brain morphology between *Shank2*$^{+/+}$ and *Shank2*$^{-/-}$ mice at the age of 8 weeks. No major differences were evident in the neuroanatomical organization of the (a) AON, (b) Amy, (c) LS, (d) MPOA, (e) VTA, and (d) NAcc. AOM, anterior olfactory nucleus medial part; AOP, anterior olfactory nucleus posterior part; MePD, medial amygdaloid nucleus, posterodorsal part; MePV, medial amygdaloid nucleus, posteroventral part; BMA, basomedial amygdaloid nucleus, anterior part; LSD, lateral septal nucleus, dorsal part; LSI, lateral septal nucleus, intermediate part; LSV, lateral septal nucleus; aca, anterior commissure, anterior part; MPOL, medial preoptic nucleus, lateral part; MPOA, medial preoptic area; SNR, substantia nigra, reticular part; VTA, ventral tegmental area; AcbC, accumbens nucleus, core; AcbSh, accumbens nucleus, shell; LAcbSh, lateral accumbens shell.